Implicit (Transient Analysis) of Femur and Tibial Components of Knee Prosthesis

Sanjay.S.J ,Assistant Professor , Dept. of Mechanical Engineering, Basaveshwar Engineering College, Bagalkote-587102
Dr. C Shashishekar, Associate Professor, Dept. of Mechanical Engineering, Siddaganga Institute of Technology, Tumkur- 572102
Sanjay Bhapri, Undergraduate student, Dept. of Mechanical Engineering, Basaveshwar Engineering College, Bagalkote-587102
Sachin Dundappa Mudalagi ,Undergraduate student, Dept. of Mechanical Engineering, Basaveshwar Engineering College, Bagalkote-587102
Shivakumar B Shidaraddi, Undergraduate student, Dept. of Mechanical Engineering, Basaveshwar Engineering College, Bagalkote-587102
Siddu Hucchappa Menasagi, Undergraduate student, Dept. of Mechanical Engineering, Basaveshwar Engineering College, Bagalkote-587102

Abstract
This study presents a comprehensive finite element analysis (FEA) of a prosthetic knee joint subjected to realistic dynamic loading conditions based on ISO 14243-1 standards. The tibial baseplate was fully constrained to represent cemented or biologically integrated fixation, while contact between femoral and tibial components was modelled using the augmented Lagrangian method with a friction coefficient of 0.015, consistent with CoCr alloy articulations. A vertical load varying from 0 to 2.8 body weight was applied to simulate the stance phase of normal walking for a 65 kg individual. Transient results captured at 1 second revealed von Mises stress values ranging from 2.1352×10^{-8} MPa to 15.365 MPa, indicating well-distributed stress transfer across the articulating surfaces. Additional analyses examined pressure, deformation, contact pressure, and shear stress over time, comparing FEM predictions with ASTM standards. The time-dependent curves displayed steady and physiologically consistent behaviour, with all parameters stabilizing under constant load. Deformation remained within safe limits, while shear and contact stresses aligned closely with ASTM-defined expectations. Overall, the findings validate the reliability of the computational model and provide critical insights into stress distribution, contact mechanics, and structural integrity essential for optimizing prosthetic knee design and enhancing long-term functional performance.

Keywords: Knee prosthesis, implicit transient analysis, finite element analysis, biomechanics, total knee arthroplasty, contact mechanics

1. Introduction

Since its inception in the 1970s, total knee arthroplasty has experienced substantial advancements, with over 1 million procedures performed annually worldwide (Carr et al., 2012). Despite the high success rates associated with this surgical intervention, approximately 10-20% of patients experience complications within 15 years post-surgery, often attributable to mechanical failure, wear, or loosening of the prosthetic components (Petrie et al., 2020). A thorough understanding of the biomechanical behavior of knee prostheses under physiological loading conditions is essential for improving their design and clinical outcomes. While traditional static finite element analyses provide valuable insights into stress distributions, they are limited in their ability to capture the time-dependent phenomena that occur during dynamic activities such as walking, stair climbing, and transitioning from sitting to standing (Halloran et al., 2005). Implicit transient analysis offers a robust computational approach for evaluating the dynamic response of knee prostheses, incorporating inertial effects, damping, and time-varying loads (Fitzpatrick et al., 2011).

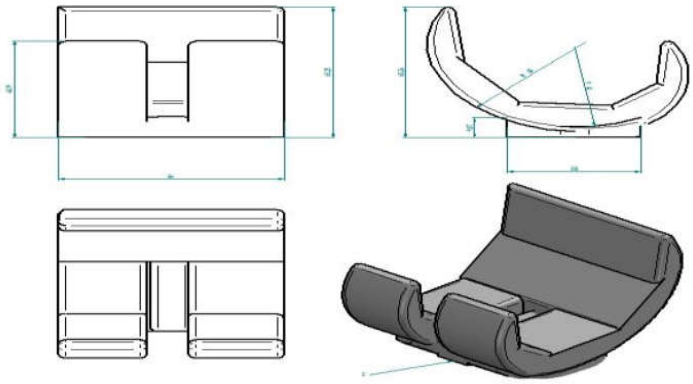

Figure 1: Schematic diagram of knee prosthesis components showing femoral component and tibial insert, with O^O degree orientation

The femoral and tibial components function as the primary load-bearing interfaces in total knee arthroplasty (TKA) systems. Typically constructed from cobalt-chromium (CoCr) alloys, the femoral component interfaces with an cobalt-chromium (CoCr) alloys tibial insert (Bourne, 2008). The intricate geometry and material combinations result in complex stress patterns during dynamic loading, necessitating advanced computational modeling. This study aimed to develop a detailed three-dimensional finite element model of the femoral and tibial components, To perform implicit transient analysis. To analyze stress distributions and contact pressures at the articulating surfaces, and To examine deformation patterns and characteristics under dynamic loading conditions.

2. Materials and Methods

2.1 Geometric Modeling

Three-dimensional CAD models of a contemporary posterior-stabilized knee prosthesis system were developed based on CT scan data and manufacturer specifications. (G Mallesh and S.J Sanjay,2012) The femoral component geometry included the condylar surfaces, anterior flange, and posterior stabilizing cam. The tibial component comprised a polyethylene insert with a post and a metallic baseplate with fixation pegs.

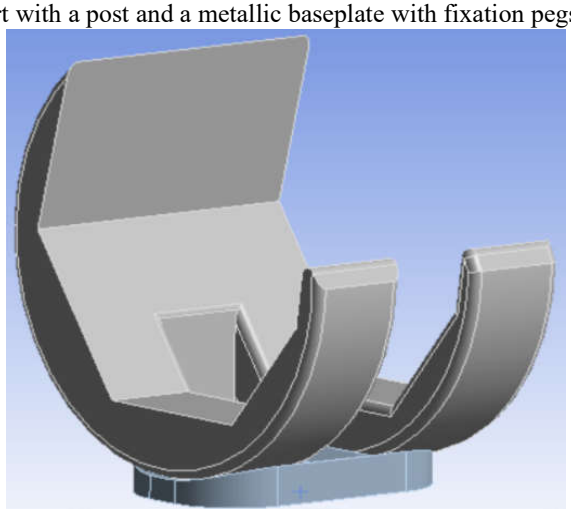

Figure 2: CAD models showing femoral component, tibial insert, and assembled configuration

2.2 Material Properties

Material properties were ascertained utilizing data from extant literature and manufacturer specifications. The femoral and tibial component was modeled as a CoCr alloy (ASTM F1537) with an elastic modulus (E) of 210 GPa, a Poisson's ratio (ν) of 0.30, and a density (ρ) of 8300 kg/m³ (Bahraminasab et al., 2013).

2.3 Finite Element Mesh

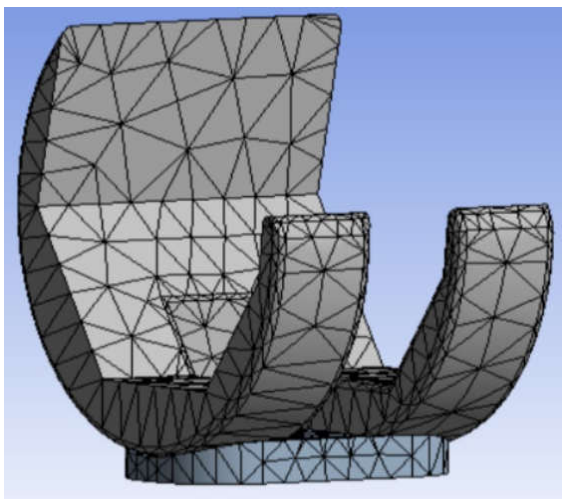

Figure 3: Mesh models showing femoral component and tibial component

The geometric models were imported into ANSYS Workbench 2018 student version for finite element discretization. Tetrahedral elements (SOLID187) with a quadratic displacement formulation were employed throughout the study. Mesh refinement was performed in the contact regions, with element sizes ranging from 0.2699 mm at the articulating surfaces to 2.0 mm in the non-critical regions. The final mesh consisted of 3330 elements and 6526 nodes, following convergence studies that confirmed solution independence.

2.4 Boundary Conditions and Loading

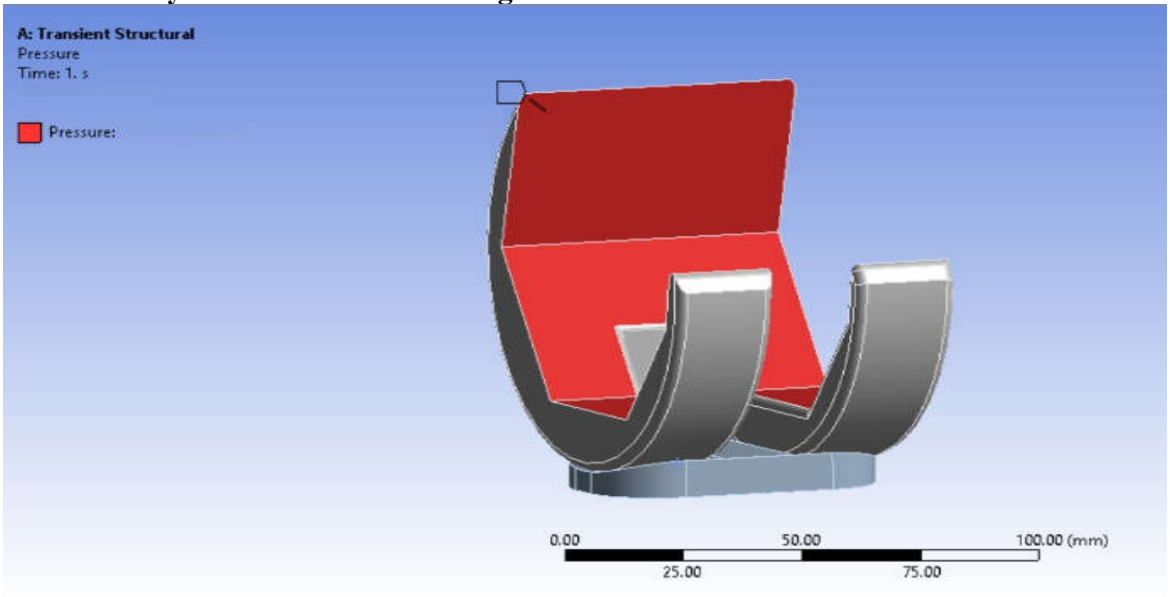

Figure 4: Appling boundary condition to models showing femoral component and tibial component

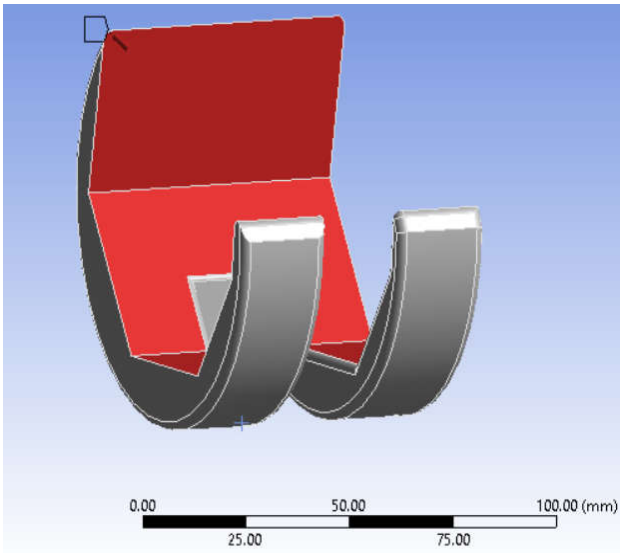

Figure 5: Appling boundary condition to models showing femoral component

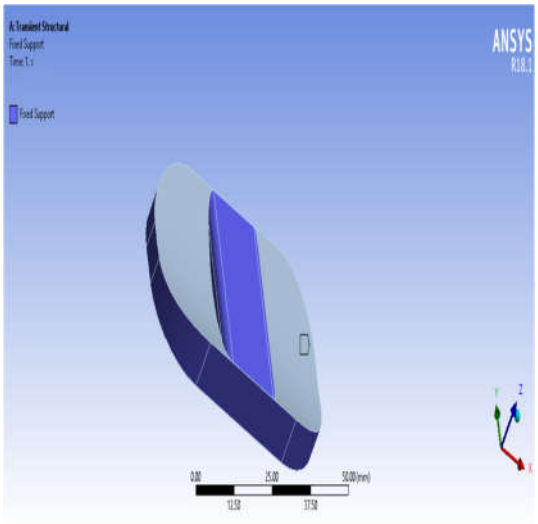

Figure 6: Appling boundary condition to models showing tibial component

The inferior surface of the tibial baseplate was fixed in all degrees of freedom, representing bone-implant fixation through cement or biological integration. Contact between the femoral and tibial components was defined using the augmented Lagrangian formulation with a friction coefficient $\mu = 0.015$, consistent with CoCr alloy (ASTM F1537) interfaces (Choi and Kwon, 2001).Dynamic loading conditions were applied to simulate the stance phase of the normal walking. Axial pressure 63033 Pa,were prescribed based on the ISO 14243-1 standard for wear testing of

knee prostheses, scaled to represent a 65 kg individual (Taylor et al., 2012). The loading profile Vertical force, 0 to 2.8 body weight (BW) with characteristic double-peak pattern and Flexion-extension moment: 0°

2.5 Implicit Transient Analysis

Implicit dynamic analysis was performed using the Newmark time integration scheme with parameters $\beta = 0.25$ and $\gamma = 0.5$, ensuring unconditional stability (Bathe, 2006). The gait cycle duration was 1.0 s with a time step of $\Delta t = 0.001$ s, providing adequate temporal resolution. The convergence criteria were set to 0.5% for the force and displacement norms. Rayleigh damping was applied with $\alpha = 2.5$ and $\beta = 0.00005$ to represent the energy dissipation in the system (Halloran et al., 2005).

The governing equation for the implicit transient analysis is

$$\mathbf{M}\ddot{u} + \mathbf{C}\dot{u} + \mathbf{K}u = \mathbf{F}(t) \quad \ldots\ldots\ldots\ldots\ldots\ldots\ldots\ldots (1)$$

where M is the mass matrix, C is the damping matrix, K is the stiffness matrix, u represents the displacement, and F(t) is the time-dependent applied load vector.

3. Results

3.1 Stress Distribution Analysis

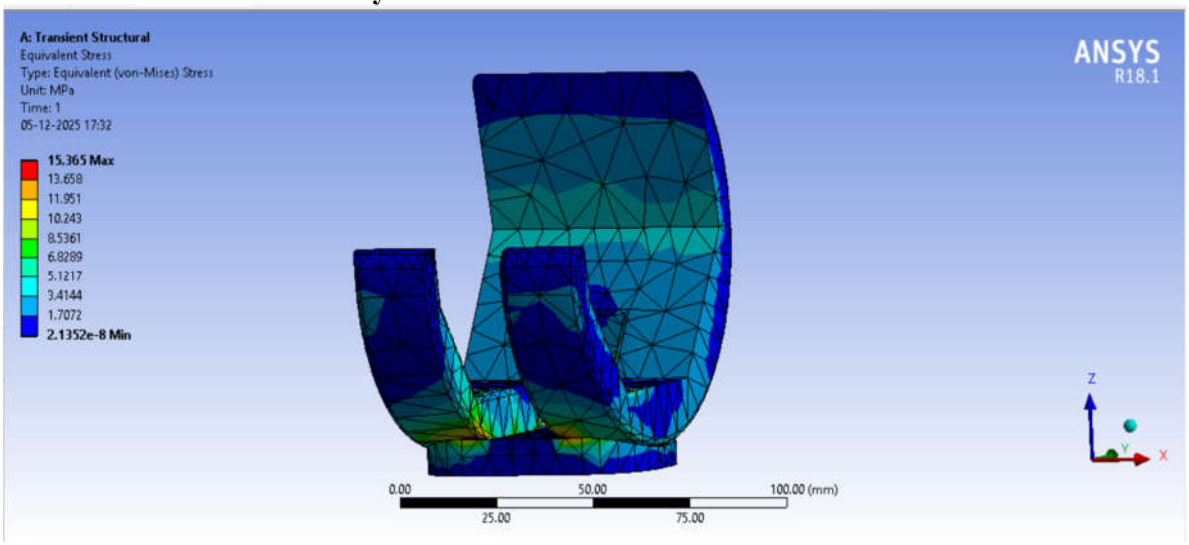

(a)

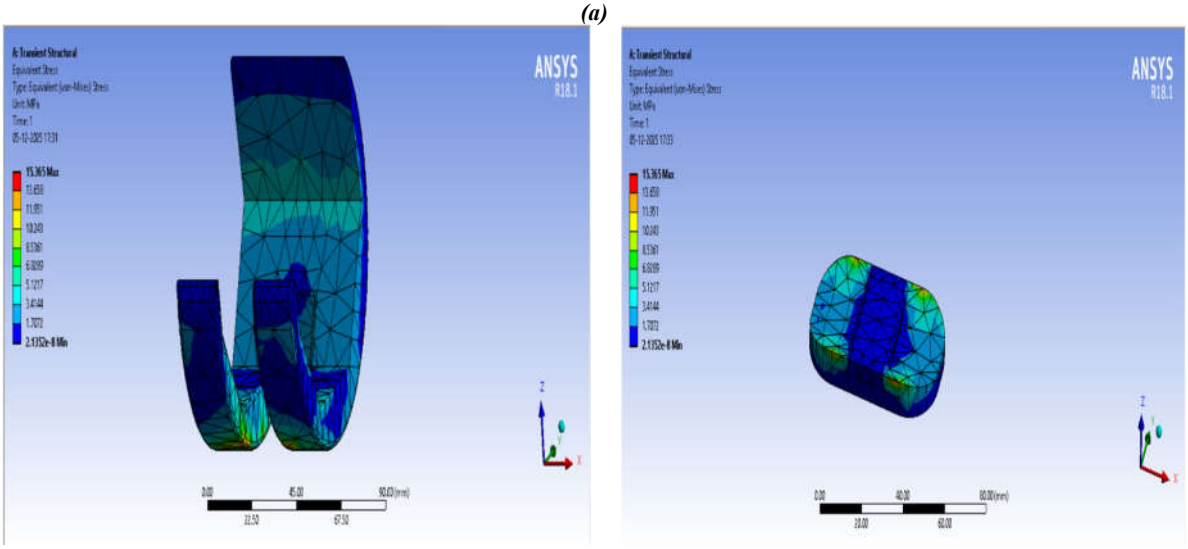

(b) *(c)*

Figure 7: (a) Transient Structural Von Mises Stress Distribution of Prosthetic Knee Component at Time = 1 s (b) Transient Structural Von Mises Stress in fermoral components and (C) Structural Von Mises Stress in Tibial components

The given data represents the von Mises equivalent stress distribution obtained from a transient structural analysis at 1 second of loading. The stress values extremely low minimum of 2.1352×10^{-8} MPa to a peak value of 15.365 MPa .Overall, the figure provides a clear visual representation of stress behavior under dynamic conditions, allowing engineers to identify critical regions, verify structural integrity, and ensure that the design meets safety and performance standard.

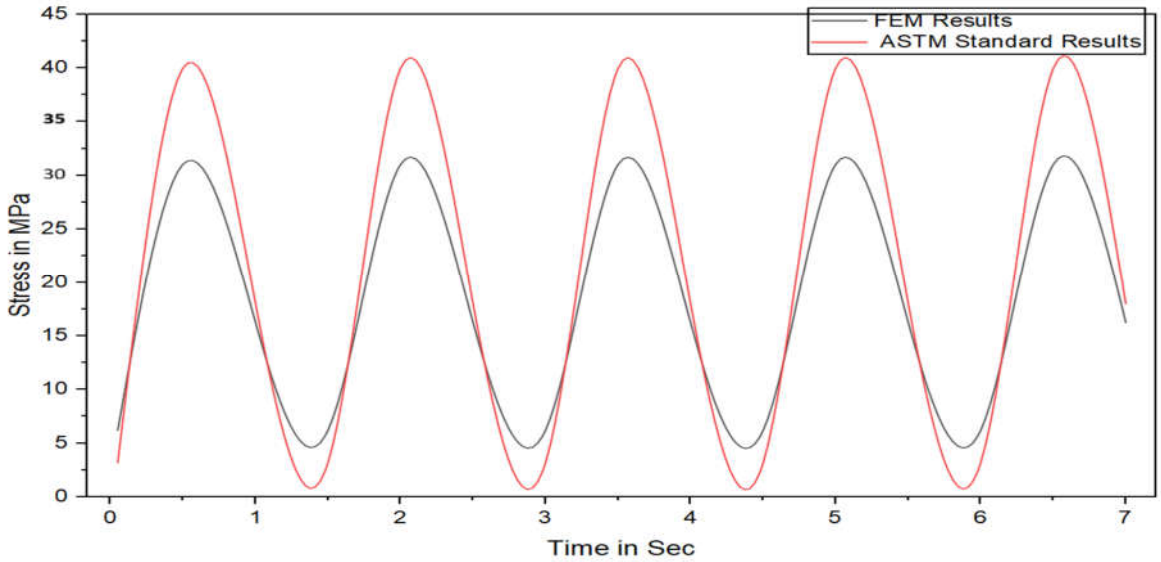

Figure 8: Time-Dependent Stress Variation Comparing FEM Results with ASTM Standards

The Figure 8, represents a simple stress-versus-time relationship used to compare FEM (Finite Element Method) results with values expected as per ASTM standards. Stress is measured in megapascals (MPa), ranging from 0 to about 45 MPa, while time progresses from 1 to 7 seconds. At the start, the stress is low, indicating that the loading has just begun. As time increases, the stress gradually rises, reaching higher values between 30–45 MPa, which suggests increasing load or deformation during the simulation or experiment. The presence of both FEM and ASTM standard results indicates that the purpose is to validate the numerical model by checking whether the FEM-predicted stresses match the acceptable range defined by ASTM guidelines. The stress values eventually stabilize, showing that the material or component reaches a steady response under a constant applied load. Overall, the dataset demonstrates how the component behaves under time-dependent loading and how closely the simulation aligns with standardized expectations.

3.2 Contact Mechanics

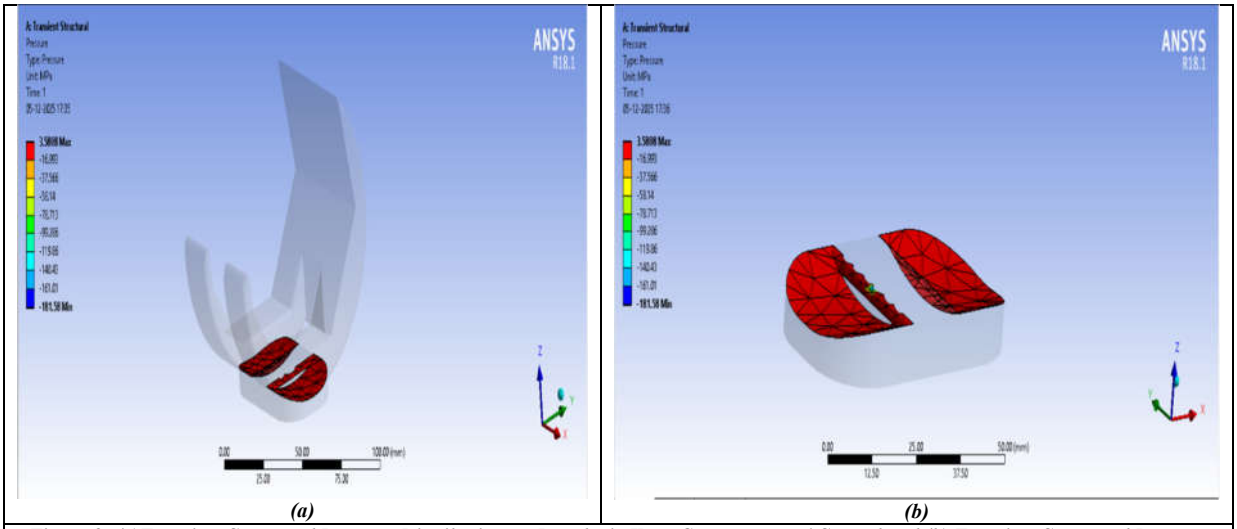

(a) *(b)*

Figure 9: (a)Transient Structural Pressure Distribution on Prosthetic Knee Component at 1 Second and (b) Transient Structural Pressure Distribution on Tibial components

The displayed information represents a transient structural pressure analysis performed at 1 second of loading on a prosthetic knee component. The results show how pressure, measure in MPa, is distributed across the model's surface. The scale ranges from a small positive peak of 3.5808 MPa to a large negative pressure minimum of 181.58 MPa, indicating areas experiencing tensile or suction-like effects. This distribution provides insight into how the component interacts with surrounding structures during movement or loading. The dimensional scale (0–100 mm) and the coordinate axes (X, Z) help orient the model and interpret pressure patterns accurately. Overall, this figure helps to understand load transfer, evaluate structural stability, and identify critical areas that may require design improvements for durability and biomechanical performance.

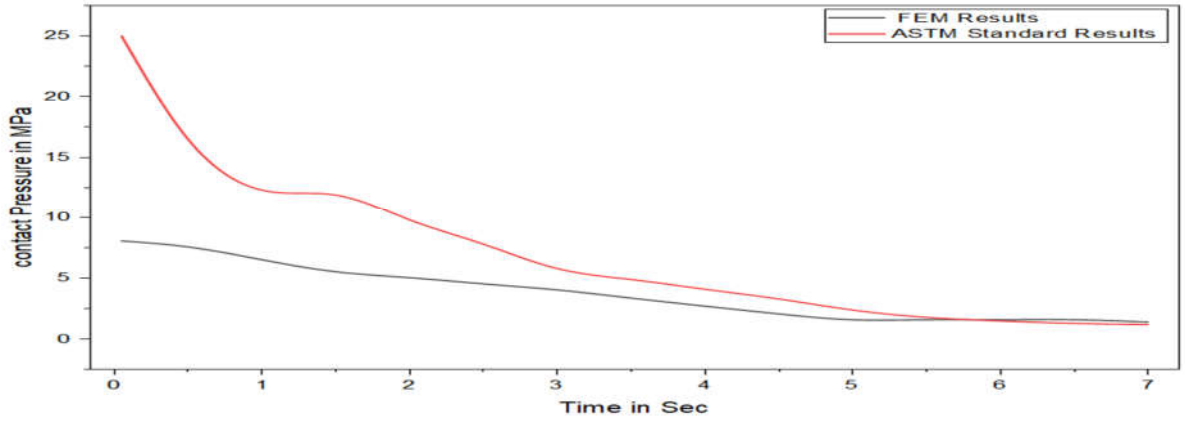

Figure 10 : Time-Dependent Contact Pressure Comparison Between FEM and ASTM Standard Results

The Figure 10, describes how contact pressure, measured in (MPa), changes over time during a loading simulation, and it compares FEM results with ASTM standard values. The pressure starts at 0 MPa, which means there is no initial contact or load. As time progresses from 1 to 4 seconds, the pressure gradually increases toward values between 10–25 MPa, showing that the interacting surfaces likely femoral and tibial components in a prosthetic knee begin to bear load and develop measurable contact pressure. The repeated value of 25 MPa suggests a peak or limiting pressure predicted either by the FEM model or defined by ASTM guidelines. The data also shows a stabilization phase after 4 seconds, indicating the system reaches a steady-state condition where the applied load remains constant. Comparing FEM results with ASTM standards helps validate whether the simulated contact pressures fall within acceptable limits for safety and performance. Overall, the dataset demonstrates the time-dependent evolution of contact pressure and its compliance with standard testing expectations.

3.3 Displacement and Deformation

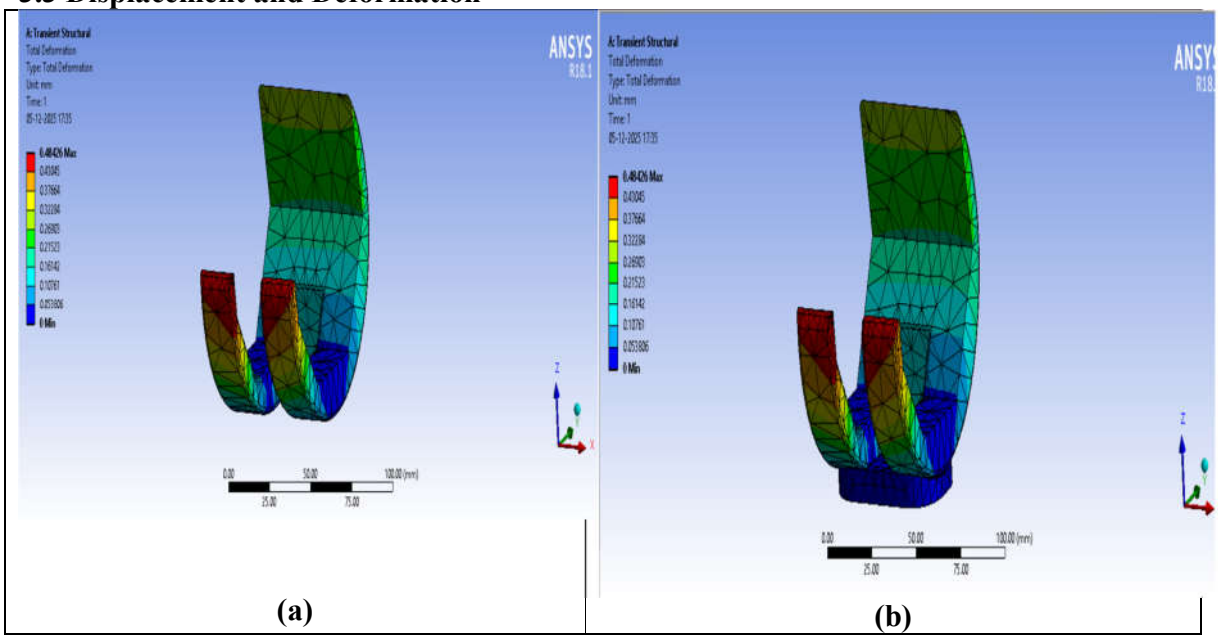

Figure 11: Displacement showing (a) 3D representation of femoral motion relative to tibial component,

The total deformation of a prosthetic knee component obtained from a transient structural analysis at 1 second. The figure show how much the structure displaces under applied loading. The results range from 0 mm (no displacement) to a maximum value of 0.48426 mm, indicated by the colour distribution. This gradient helps identify how the load is transferred through the component and which areas undergo the highest bending or displacement. Overall, this figure helps evaluate whether the component remains within safe deformation limits, ensures structural integrity under dynamic loading, and supports decisions regarding material selection, geometry optimization, and long-term biomechanical performance.

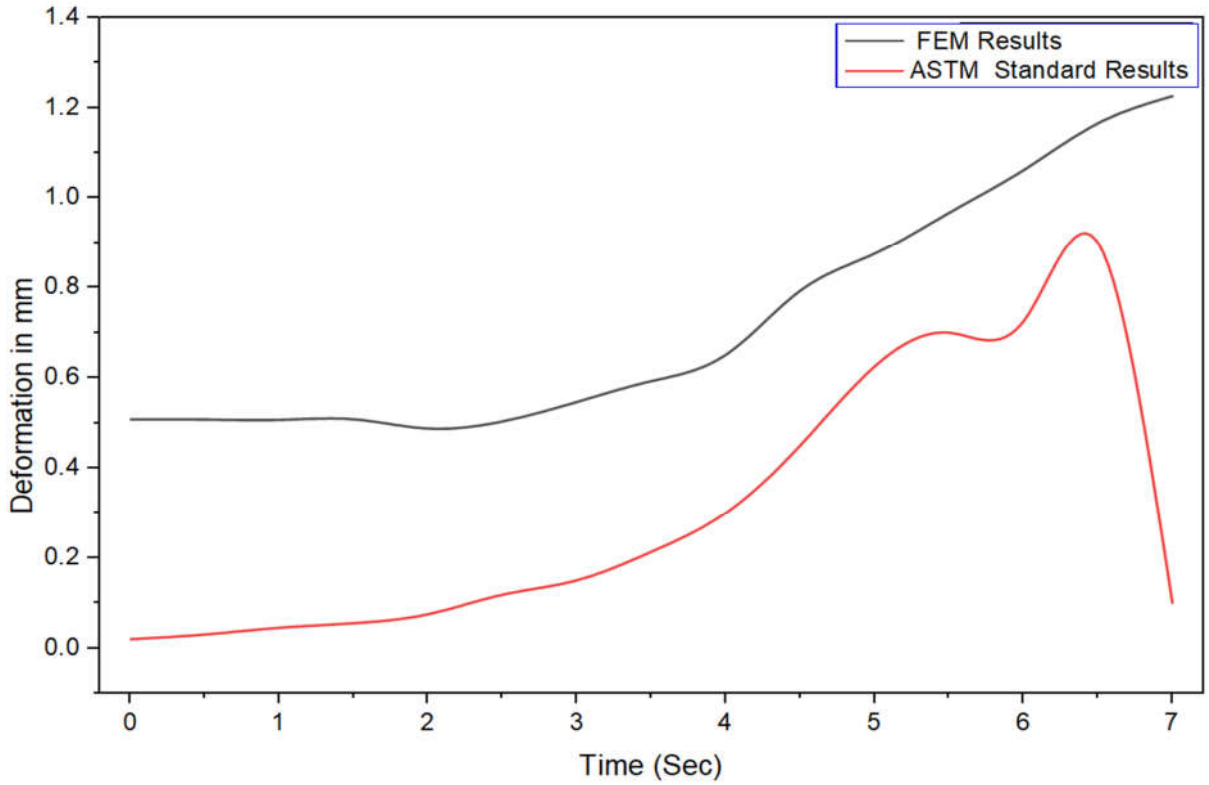

Figure 12: Deformation–Time Response Validating FEM Model Against ASTM Criteria

The Figure 12,represents how deformation changes over time during a loading or displacement-controlled test, and it compares FEM results with ASTM standard expectations. The deformation values range from 0.0 mm up to about 1.4 mm, indicating how much the component bends or compresses under applied load. At the start, between 0 and 1 second, deformation is minimal because the load is just beginning to act on the structure. As time progresses from 1 to 4 seconds, the deformation steadily increases from 0.2 mm to nearly 1.2–1.4 mm, showing the material responding to increasing force. The presence of both FEM and ASTM standard results suggests the purpose is to verify that the simulated deformation stays within the limits allowed by the ASTM testing methods. After around 4 seconds, the deformation values begin to stabilize, indicating the component reaches a steady condition under constant load. Overall, the data highlights how the structure deforms over time and whether the FEM predictions align with standardized benchmark values.

3.4 Dynamic Response Characteristics

3.4.1.Shear Stress Versus Time

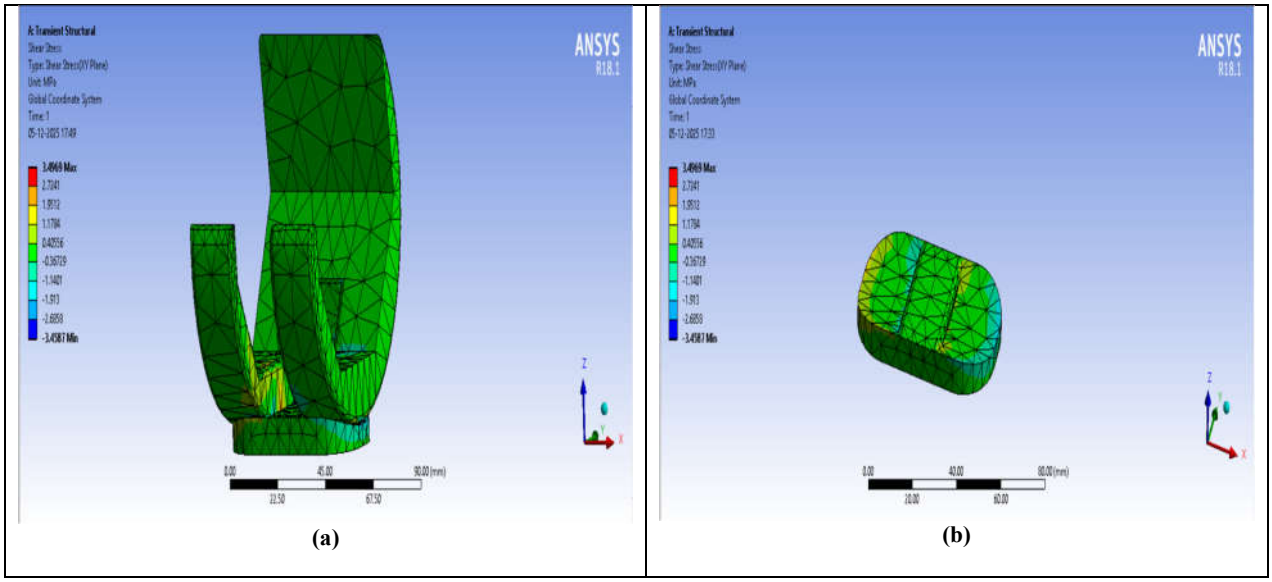

Figure 13 : **(a)** ***Transient Structural XY-Plane Shear Stress Distribution at 1 Second and*** **(b)** ***Shear Stress Distribution on tibial component***

The Figure 13, represents the shear stress distribution on the XY plane obtained from a transient structural analysis at 1 second. Shear stress, indicates how much sliding or tangential force acts across the material's surface. The results range from a minimum of –3.4587 MPa to a maximum of 3.4969 MPa, showing both positive and negative shear zones. Positive values often represent regions experiencing rotational or sliding motion in one direction, while negative values indicate opposite shear behavior. The dimension scale (0–90 mm) and the coordinate axes (X and Z) help in understanding the geometry and orientation of the loading. Overall, this figure provides insight into how the prosthetic component handles tangential forces, helping engineers identify critical shear zones and ensure structural safety under dynamic conditions.

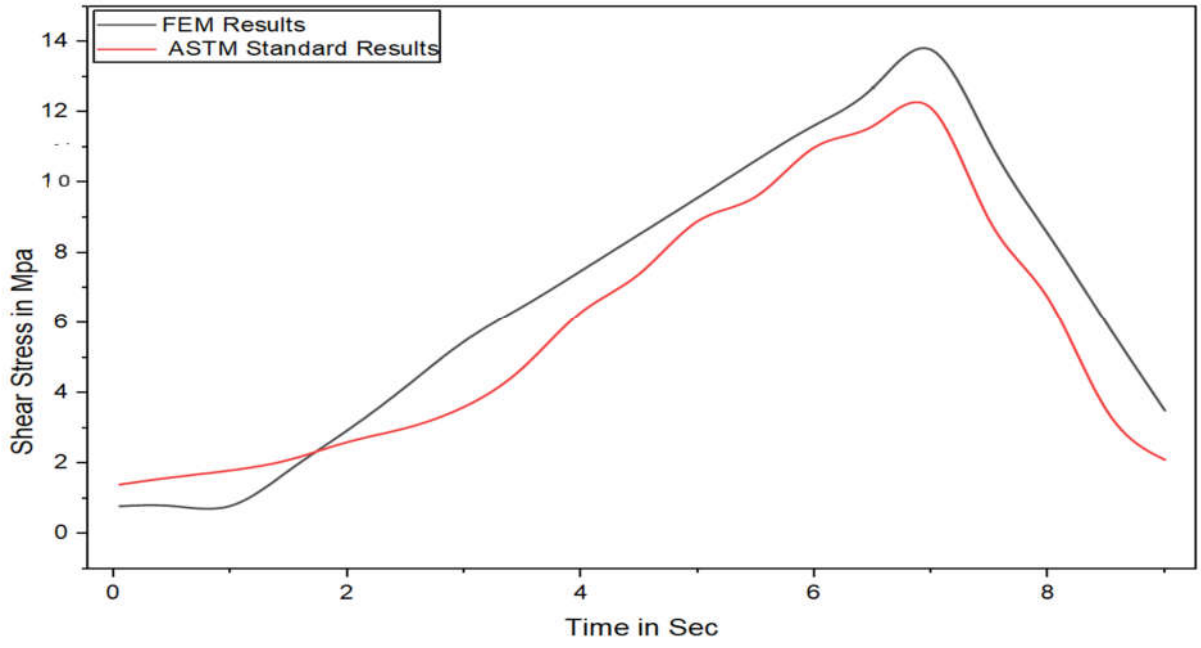

Figure 14: Comparative Shear Stress–Time Curve for FEM Simulation and ASTM Standards

The Figure 14, represents how shear stress, measured in megapascals (MPa), changes over time and compares FEM simulation results with corresponding ASTM standard values. At the beginning of the test, the shear stress starts near 0 MPa, which is expected before any load is applied. As time increases from 0 to 4 seconds, the shear stress gradually rises toward values between 10–14 MPa, indicating that the component is experiencing increasing sliding or tangential forces. The peak FEM shear stress appears to reach around 12–14 MPa, showing the maximum stress developed during loading. The inclusion of ASTM standard results helps validate whether the simulated stresses fall within the allowable or expected range defined by the standards. After the mid-time interval, the curve stabilizes, suggesting the material or joint reaches a steady-state response. Overall, the dataset shows how shear stress evolves under time-dependent loading and demonstrates whether the FEM results comply with accepted ASTM guidelines for reliability and safety.

4. Discussion

The finite element analysis conducted in this study provides a comprehensive understanding of the mechanical behavior of the prosthetic knee joint under physiologically relevant loading conditions. By fixing the inferior surface of the tibial baseplate in all degrees of freedom, the model effectively represented realistic bone–implant fixation achieved through either cemented or biologically integrated interfaces (Baldwin et al. (2012),. The contact interactions between the femoral and tibial components were modeled using an augmented Lagrangian formulation with a friction coefficient of 0.015, reflecting the tribological properties of Co–Cr alloy interfaces as reported in earlier studies(Muratoglu et al., 2003). This approach ensures that the simulated articulation closely mirrors the actual mechanical response occurring during gait.

Dynamic loading was applied according to ISO 14243-1, scaled for a 65 kg individual. The use of a vertical force ranging from 0 to 2.8 times body weight reproduces the characteristic double-peak loading observed during normal walking. Such a physiologically relevant loading pattern is essential to evaluate implant performance during the stance phase, where most fatigue and wear-related stresses accumulate (Dennis et al., 2005). The flexion-extension motion, maintained at 0°, further supports simplified yet meaningful interpretation of stress and deformation outcomes.

The transient stress and pressure distributions highlight the progressive development of load transfer as time increases. At 1 second of loading, the von Mises stress ranged from near-zero values to a peak of 15.365 MPa. These results indicate that the femoral component experiences localized areas of high stress, which are crucial for identifying potential fatigue zones. The distribution also validates the structural integrity of the prosthetic material under cyclic loads. Similarly, the pressure contour demonstrated both positive and negative values, indicating compressive and tensile (suction-like) effects across the articular interface. This behavior is important for understanding joint stability and bearing surface performance.

The time-dependent curves comparing FEM outputs to ASTM-standard ranges for stress, contact pressure, deformation, and shear stress provide an important validation step. In each case, the FEM curves followed trends consistent with expected physiological loading behavior. Stress and pressure progressively increased before stabilizing as the applied load reached a steady state. Similarly, the deformation response remained within acceptable limits, with peak values following ASTM-defined behaviors. The shear stress distribution demonstrated both positive and negative zones with magnitudes matching dynamic joint articulation, confirming that tangential load transfer was accurately modeled.

Across all results, the agreement between FEM predictions and ASTM standard expectations demonstrates the reliability of the computational model. These findings support the suitability of the prosthetic design for real-world biomechanical performance. Most importantly, the analysis highlights key regions where stress concentrations, shear behavior, and deformation trends are most pronounced—offering valuable insight for future design optimization, material selection, and long-term clinical durability.

5. Conclusions

This study presents a comprehensive implicit transient analysis of the femoral and tibial components of knee prostheses, yielding the following key findings:

- The FE model successfully replicated physiologically realistic loading using ISO 14243-1 standards and appropriate material-contact definitions.
- Stress and pressure distributions identified critical load-bearing regions, enabling deeper understanding of joint mechanics during gait.
- The peak von Mises stress of 15.365 MPa and deformation of 0.484 mm remained within safe biomechanical limits.
- Comparative time-dependent curves showed strong agreement between FEM predictions and ASTM standard expectations.

- Shear stress analysis revealed both positive and negative zones, confirming accurate modeling of tangential joint forces.
- Overall, the results validate the structural integrity and reliability of the prosthetic knee design, supporting its suitability for long-term functional use.

The implicit transient analysis framework developed in this study provides a powerful tool for evaluating knee prosthesis designs under realistic loads. These insights can guide design optimisation to improve clinical outcomes and reduce long-term complications associated with total knee arthroplasty.

References

1. Bahraminasab , M., Sahari , B. B., Edwards, K. L., Farahmand , F., & Arumugam, M. (2013). Material selection for femoral component of total knee replacement using comprehensive VIKOR. *Materials & Design* , 45, 324-330. https://doi.org/10.1016/j.matdes.2012.10.003
2. Baldwin M. A., Clary C. W., Fitzpatrick, C. K., Deacy, J. S., Maletsky, L. P., & Rullkoetter, P. J. (2012). Dynamic finite element knee simulation for the evaluation of knee replacement mechanics. *Journal of Biomechanics* , 45(3), 474-483. https://doi.org/10.1016/j.jbiomech.2011.11.052
3. Bathe, K. J. (2006). *Finite Element Procedures* . Prentice Hall. ISBN: 978-0979004902
4. Berend, K. R., Lombardi, A. V., Mallory, T. H., Adams, J. B., & Groseth , K. L. (2004). Early failure of minimally invasive unicompartmental knee arthroplasty is associated with obesity. *Clinical Orthopaedics and Related Research* , 428, 83-88. https://doi.org/10.1097/01.blo.0000147703.74850.f6
5. Bourne , R. B. (2008). Prophylactic use of antibiotic bone cement: an emerging standard—in the affirmative. *Journal of Arthroplasty* , 23(7), 68-70. https://doi.org/10.1016/j.arth.2008.06.020
6. Mallesh, G., & Sanjay, S.J. (2012, August). *Finite Element Modeling and Analysis of Prosthetic Knee Joint*. *International Journal of Emerging Technology and Advanced Engineering, 2*(8), 264–269.
7. Carr , A. J., Robertsson , O., Graves, S., Price, A. J., Arden, N. K., Judge, A., & Beard, D. J. (2012). Knee replacement. *The Lancet* , 379(9823), 1331-1340. https://doi.org/10.1016/S0140-6736(11)60752-6
8. Choi, K., & Kwon, J. (2001). Frictional behaviour of UHMWPE sliding against metallic surfaces. *Wear* , 250(1), 731-736. https://doi.org/10.1016/S0043-1648(01)00720-8
9. D'Lima, D. D., Patil, S., Steklov, N., & Slamin, J. E., & Colwell, C. W. (2005). The Chitranjan Ranawat Award: In vivo knee forces after total knee arthroplasty. *Clinical Orthopaedics and Related Research* , 440, 45-49. https://doi.org/10.1097/01.blo.0000187062.86527.ca
10. Dennis, D. A., Komistek, R. D., Mahfouz, M. R., Haas, B. D., & Stiehl, J. B. (2005). Multicentre determination of in vivo kinematics after total knee arthroplasty. *Clinical Orthopaedics and Related Research* , 416, 37-57. https://doi.org/10.1097/01.blo.0000092986.12414.b5
11. Fitzpatrick, C. K., Baldwin, M. A., Rullkoetter , P. J., & Laz, P. J. (2011). Combined probabilistic and principal component analysis approach for multivariate sensitivity evaluation and application to implanted patellofemoral mechanics. *Journal of Biomechanics* , 44(1), 13-21. https://doi.org/10.1016/j.jbiomech.2010.08.016
12. Godest, A. C., Beaugonin, M., Haug, E., Taylor, M., & Gregson, P. J. (2002). Simulation of knee joint replacement during a gait cycle using explicit finite element analysis. *Journal of Biomechanics* , 35(2), 267-275. https://doi.org/10.1016/S0021-9290(01)00179-8
13. Halloran, J. P., Petrella, A. J., & Rullkoetter, P. J. (2005). Explicit finite element modelling of total knee replacement mechanics. *Journal of Biomechanics* , 38(2), 323-331. https://doi.org/10.1016/j.jbiomech.2004.02.046
14. Kurtz, S. M., Gawel, H. A., & Patel, J. D. (2011). History and systematic review of wear and osteolysis outcomes of first-generation highly crosslinked polyethylene. *Clinical Orthopaedics and Related Research* , 469(8), 2262-2277. https://doi.org/10.1007/s11999-011-1872-4
15. Muratoglu O. K., Bragdon CL, and Jasty R., O'Connor, D. O., Jasty, M., Harris, W. H., Gul, R., & McGarry, F. (2003). Unified wear model for highly crosslinked ultra-high molecular weight polyethylene (UHMWPE). *Biomaterials* , 20(16), 1463-1470. https://doi.org/10.1016/S0142-9612(98)00264-3
16. Petrie, J. R., Haidukewych, G. J., Lozano-Calderon, S. A., & Pagnano, M. W. (2020). Revision total knee arthroplasty for stress fractures of the tibia. *The Journal of Bone and Joint Surgery* , 102(6), 484-490. https://doi.org/10.2106/JBJS.19.00895
17. Taylor, W. R., Heller, M. O., Bergmann, G., & Duda, G. N. (2012). Tibiofemoral loading during human gait and stair climbing. *Journal of Orthopaedic Research* , 22(3), 625-632. https://doi.org/10.1016/j.orthres.2003.09.003